0022-1767/88/1414-1137$02.00/0
THE JOURNAL OF IMMUNOLOGY

Vol. 141, 1137–1142, No. 4, August 15, 1988
Printed in U.S.A.

ABUNDANT EXPRESSION OF TYPE *l* K^+ CHANNELS

A Marker for Lymphoproliferative Diseases?[1]

STEPHAN GRISSMER,* MICHAEL D. CAHALAN,* AND K. GEORGE CHANDY*†,[2]

*From the *Department of Physiology and Biophysics and † Division of Basic and Clinical Immunology, Department of Medicine, University of California, Irvine, CA 92717*

Using the patch clamp whole-cell recording technique, we studied expression of K^+ channels in mAb-defined T cell subsets from diseased C3H-*lpr/lpr* and C3H-*gld/gld* mice and from healthy C3H-HeJ congenic controls. Both mutant mouse strains develop a lupus-like syndrome accompanied by hyperplasia of a functionally and phenotypically abnormal T cell subset. These defective cells, which are Thy-1.2$^+$ CD4$^-$ CD8$^-$ B220$^+$ F23.1$^+$, display an abundance of type *l* K^+ channels. Phenotypically similar lymph node T cells from normal C3H-HeJ mice, or young C3H-*lpr/lpr* mice before the onset of disease, do not display large numbers of type *l* K^+ channels. CD4$^+$ CD8$^-$ T cells (helper/inducer) from the mutant mice express a small number of type *n* K^+ channels, and CD4$^-$ CD8$^+$ T cells (suppressor/cytotoxic) show a low level of type *l* or *n'* K^+ channels, as do their phenotypically equivalent counterparts in the normal mouse thymus. These results suggest that the abundant expression of type *l* K^+ channels is a marker for the defective *lpr* and *gld* T cell subset and may reflect the "abnormal" proliferative status of these cells.

At least three types of voltage-gated K^+ channels, termed *n*, *n'*, and *l*, are expressed by murine T cells (1–3). These K^+ channels can be distinguished on the basis of their pharmacology, kinetics, voltage dependence, and single-channel conductance (1–3). Normal murine resting lymph node T cells express small numbers (~10 to 20 channels/cell) of one of these types of K^+ channels, whereas lymph node-derived T cells activated by the mitogen, ConA, possess about 20 times more K^+ channels (4, 5). Recently, Lewis and Cahalan (2, 3) reported that CD4$^+$ CD8$^-$ thymocyte subsets (helper/inducer) express type *n* K^+ channels (20 to 100/cell), whereas CD4$^-$ CD8$^+$ thymocytes (suppressor/cytotoxic) display type *l* or *n'* K^+ channels (20 to 200/cell). Thus, K^+ channel expression could be used as a marker to distinguish T cell subsets.

MRL-MpJ mice homozygous for the autosomal recessive mutation *lpr* (denotes lymphoproliferation) develop substantial lymphadenopathy and a disease resembling SLE (6). The proliferating cells in these hyperplastic organs express the TCR (7–10) and the Thy-1 marker, indicating T cell lineage (8, 11–13). However, unlike mature T cells, these cells do not express either the CD4 or the CD8 T cell differentiation markers (8, 13, 14), and they additionally express a pre-B cell marker, Ly-5 or B220 (8, 13). These cells have been suggested to represent an immature T cell subset. The *lpr* gene locus has been introduced into different murine genetic backgrounds (e.g. C3H-HeJ-*lpr/lpr*, C57B1-6J-*lpr/lpr*) (15, 16). All mouse strains expressing the *lpr* mutation develop lupus accompanied by hyperplasia of T cells with the same unique cell surface phenotype (15). The chromosome location of the mutant gene *lpr* has not been mapped (17).

Another mutation, *gld* (generalized lymphoproliferative disease), also induces hyperplasia of T cells phenotypically and functionally identical to the expanded subset in MRL-MpJ-*lpr/lpr* mice (8, 17–19), along with lupus-like disease. The location of this mutant gene has been mapped to chromosome 1 approximately 10 centimorgan from the dominant loop tail gene *lp* (17).

We previously reported that the majority of lymph node T cells from diseased MRL-MpJ-*lpr/lpr* mice express a large number of type *l* K^+ channels (20). The *lpr* mutation is the first example of a genetic defect associated with an ion channel alteration in cells of the immune system. Several interesting questions arise from this observation. 1) Does the *lpr* mutation alone, or in combination with other genes, cause altered ion channel expression in lymphocytes? 2) Would other single-gene mutations that lead to autoimmune disease and lymphoid hyperplasia result in abnormal channel expression? 3) Is the abnormal channel expression in MRL-MpJ-*lpr/lpr* T cells correlated with a specific T cell phenotype? We have addressed these questions in the present investigation.

MATERIALS AND METHODS

Mice

C3H-HeJ, C3H-HeJ-*lpr/lpr* and C3H-HeJ-*gld/gld* mice were purchased from the Jackson Laboratory (Bar Harbor, ME). One C3H-HeJ mouse, seven C3H-HeJ-*lpr/lpr* mice, and three C3H-HeJ-*gld/gld* mice were examined in the studies described in this report. The three C3H-HeJ-*gld/gld* mice and three of the seven C3H-HeJ-*lpr/lpr* mice examined were >15 wk of age and demonstrated severe lymphadenopathy. One C3H-HeJ-*lpr/lpr* mouse was 12 wk old and did not

Received for publication February 14, 1988.
Accepted for publication May 16, 1988.
The costs of publication of this article were defrayed in part by the payment of page charges. This article must therefore be hereby marked *advertisement* in accordance with 18 U.S.C. Section 1734 solely to indicate this fact.
[1] This study was supported by grants from the National Institutes of Health (AI-24783 and NS14609), the Arthritis Foundation, Southern California Chapter (AF-9488), the Office of Naval Research, and the University of California at Irvine Faculty Research Grant (505139-19900). S. G. is supported by a Deutsche Forschungsgemeinschaft research fellowship (Gr 848/2-2).
[2] Please address all correspondence and requests for reprints to Dr. K. George Chandy, Room C-302, Division of Basic and Clinical Immunology, Department of Medicine, University of California at Irvine, Irvine, CA 92717.

exhibit clinically identifiable lymphadenopathy. Three C3H-HeJ-*lpr*/*lpr* mice were 2 to 5 wk old and did not show any signs of disease.

Antibodies

PE[3]-conjugated-anti-CD4 (L3T4) and FITC-conjugated-anti-CD8 (Lyt-2) antibodies were purchased from Becton Dickinson (Mountain View, CA). Anti-Thy-1.2 and anti-B220 (RA3-6B2) were purified from ascites in our laboratory. The TCR V_β8-chain-specific mAb F23.1 (21), was a generous gift from Dr. R. P. Shimonkevitz (Research Institute of Scripps Clinic, La Jolla, CA); the antibody reacts with all three members of the V_β8 family. Fluoresceinated goat anti-mouse IgG antibody (affinity purified and absorbed with rat Ig) and PE-conjugated goat anti-rat IgG (affinity purified and absorbed against mouse Ig) were purchased from Caltag (Rupp and Bowman, Tustin, CA).

Separation of T Cells

Mice were killed, and single-cell suspensions were prepared from the thymus or lymph nodes. In previous experiments, we had observed that the $g_{k,max}$ values of T cells from lymph nodes and spleen were similar; therefore, in the present study, we pooled the cells obtained from the mesenteric, inguinal, and axillary lymph nodes (20). T cells were enriched by passage through a nylon wool column.

Staining

Direct staining. Cells (2×10^6) were incubated with an appropriate dilution of anti-CD4-PE and either anti-CD8-FITC or anti-Thy-1.2-FITC for 30 min on ice, washed three times, and resuspended in 1 ml of RPMI 1640 medium containing 10% heat-inactivated FCS (Hyclone, Logan, UT) and 2 mM L-glutamine. The stained cells were plated into glass chambers, and the major T cell subsets were then identified by epifluorescence microscopy. When anti-CD4 and anti-CD8 antibodies were used, three populations were evident: orange ($CD4^+$ $CD8^-$), green ($CD4^-$ $CD8^+$), and unstained ($CD4^-$ $CD8^-$). When anti-Thy-1.2 and anti-CD4 antibodies were used, the Thy-1.2^+ $CD4^-$ cells appeared green, and Thy-1.2^+ $CD4^+$ cells were yellow. Ion channel expression was then characterized in these cells. In most experiments, chambers were coated with polylysine (0.5 mg/ml) to improve cell adherence to the dish. This procedure did not alter channel expression when compared with cells plated into uncoated glass chambers.

Counterstaining. In some experiments, patch-clamped $CD4^-$ $CD8^-$ cells, still attached to the recording pipette, were counterstained with anti-TCR antibody (F23.1) for 10 min, washed with mammalian Ringer, incubated for a further 10 min with goat anti-mouse IgG-FITC, washed again with mammalian Ringer, and then visualized by epifluroescence microscopy. Subsequently, the cell was similarly incubated with anti-B220 followed by goat anti-rat IgG-PE. In two experiments, the patch-clamped cell was first stained with B220 and then with F23.1.

Identification of a $CD4^-$ $CD8^-$ $B220^-$ F23.1^+ T cell subset. Lymph node T cells from normal C3H-HeJ mice were purified on two successive nylon wool columns to remove contaminating B cells. These cells (2×10^6 cells) were first incubated with an appropriate dilution of anti-TCR antibody (F23.1) for 20 min on ice and then washed three times with medium. They were then incubated with goat anti-mouse IgG-FITC, which binds F23.1 antibody, for 20 min, and then washed three times with medium. Next, the cells were incubated for 20 min with anti-CD4, anti-CD8, and anti-B220 antibodies, washed three times with medium, and then incubated for a further 20 min with goat anti-rat IgG-PE (binds anti-CD4, anti-CD8, and anti-B220 antibodies). The cells were washed three times with medium and resuspended in 1 ml of medium. Only F23.1^+ $CD4^-$ $CD8^-$ $B220^-$ cells (green cells) were voltage clamped. The remainder of the cells, which were orange, yellow, or unstained, were not examined. Contaminating B cells (surface Ig^+ and $B220^+$) were excluded from the voltage clamp analyses because these cells would be yellow.

Electrophysiologic Experiments

After phenotypic identification by epifluorescence microscopy, single T cells were voltage clamped by using the whole-cell recording mode of the patch clamp technique. Details of the gigohm-seal voltage clamp technique used here are described elsewhere (22). All experiments were done at room temperature (22 to 26°C).

Solutions. The cells under investigation were bathed in normal mammalian Ringer solution (160 mM NaCl, 4.5 mM KCl, 2.0 mM $CaCl_2$, 1.0 mM $MgCl_2$, 5 mM HEPES, adjusted to pH 7.4 with NaOH; 290 to 320 mosm). In Ringer solutions containing TEA chloride (TEA^+), NaCl was replaced by appropriate TEA^+ concentrations, keeping the osmolarity constant. The bath solution could be changed during the recordings by bath perfusion. The patch pipette usually contained 134 mM KF, 11 mM EGTA, 1 mM $CaCl_2$, 2 mM $MgCl_2$, 5 mM HEPES, adjusted to pH 7.2 with KOH; 285 to 310 mosm.

Data acquisition. The holding potential was adjusted in all experiments to −80 mV. The patch clamp amplifier (List L/M-EPC 7) was used in the voltage clamp mode without series resistance compensation. Electrodes were pulled in three stages, coated with Sylgard (Dow Corning Corp., Midland, MI) and firepolished to resistances, measured in the bath, of 2 to 7 Mohm. In all experiments, the command input of the patch clamp amplifier was controlled by a computer (PDP 11/73) via a digital analogue converter, and membrane currents were recorded at a band width of 2 kHz. In our experiments, the recorded membrane current during depolarizations consisted of a capacitative, a linear leakage, and the specific voltage-dependent K^+ current. To study the K^+ current in isolation, we corrected for the linear leakage and capacitative currents. This was achieved by measuring a mean current associated with eight pulses delivered from a hyperpolarizing potential. At this potential, the membrane current consists only of the capacitative and leakage current inasmuch as all of the K^+ channels are closed. The mean current was then appropriately scaled and subtracted from the total membrane current measured at depolarizing potentials. All potentials were corrected for the liquid junction potential that develops at the tip of the pipette if the pipette solution is different from that of the bath. The liquid junction potential between the normal internal (pipette) and external (bath) solution was −7 mV.

Selection of cells for recording. Normal T cells increase in size upon activation and express large numbers of type *n* K^+ channels (5). In unstimulated lymphoid populations, large cells (>8 μm) express large numbers of type *n* K^+ channels and probably reflect "spontaneously activated" cells (5). To avoid clamping spontaneously activated cells, we examined cells with a capacitance <2 pF, which corresponds to a cell diameter <8 μm. The relationship between cell diameter and cell capacitance has previously been calculated to be 0.98 μF/cm² (22), assuming that lymphocytes are smooth spheres.

Identification of K^+ channel type. We identified K^+ channels on the basis of their inactivation properties, channel-closing kinetics, and sensitivity to block by TEA^+ as described elsewhere in detail (2, 3, 5). Typically, type *n* K^+ channels are use dependent, i.e., show cumulative inactivation by repetitive depolarizing pulses. We determined use dependence by measuring the decline in the size of the K^+ current elicited with one-per-second repetitive depolarizing pulses of 200-ms duration. Type *n* K^+ channels also close slowly upon repolarization with a time constant of about 30 ms at −60 mV and are blocked by TEA^+ (K_D = 8 mM). Type *l* K^+ channels are not use dependent, close more rapidly on repolariziaton with a time constant of 2 ms at −60 mV, and are much more sensitive to block by TEA (K_D = 0.1 mM). Type *n'* K^+ channels are not use dependent, close slowly like type *n* K^+ channels upon repolarization, but are less sensitive to block by TEA (K_D = ~100 mM).

Determination of maximal K^+ conductance ($g_{k,max}$) and number of K^+ channels per cell. $g_{k,max}$ was calculated from the largest K^+ current recorded in each cell. The measured reversal potential for types *n*, *n'*, and *l* K^+ channels is between −75 and −85 mV with KF in the pipette and normal Ringer on the outside (3, 22). We therefore used a reversal potential of −80 mV to calculate $g_{k,max}$. The number of K^+ channels per cell was calculated by dividing $g_{k,max}$ by the single-channel conductances of the appropriate channel type; the single-channel conductances are 18, 27, and 17 pS for *n*, *l*, and *n'*, respectively (3).

RESULTS

The lpr gene mutation causes altered ion channel expression in lymph node T cells, irrespective of the genetic strain of the mouse. C3H-*lpr*/*lpr* mice develop a lupus-like disease along with lymphoproliferation of a Thy-1.2^+ $CD4^-$ $CD8^-$ TCR^+ $B220^+$ T cell subset that is phenotypically identical to the abnormal cells in MRL-MpJ-*lpr*/*lpr* mice (8). Figure 1 shows K^+ outward currents in the major T cell subsets defined by the CD4 and CD8 markers in C3H-*lpr*/*lpr* mice. In these experiments, the membrane potential of the cells was held at −80 mV, and then depolarizing pulses were applied to +40 mV. This protocol opens all the voltage-gated K^+ channels in the

[3] Abbreviations used in this paper: PE, phycoerythrin; TEA, tetraethylammonium; $g_{k,max}$, maximal K^+ conductance.

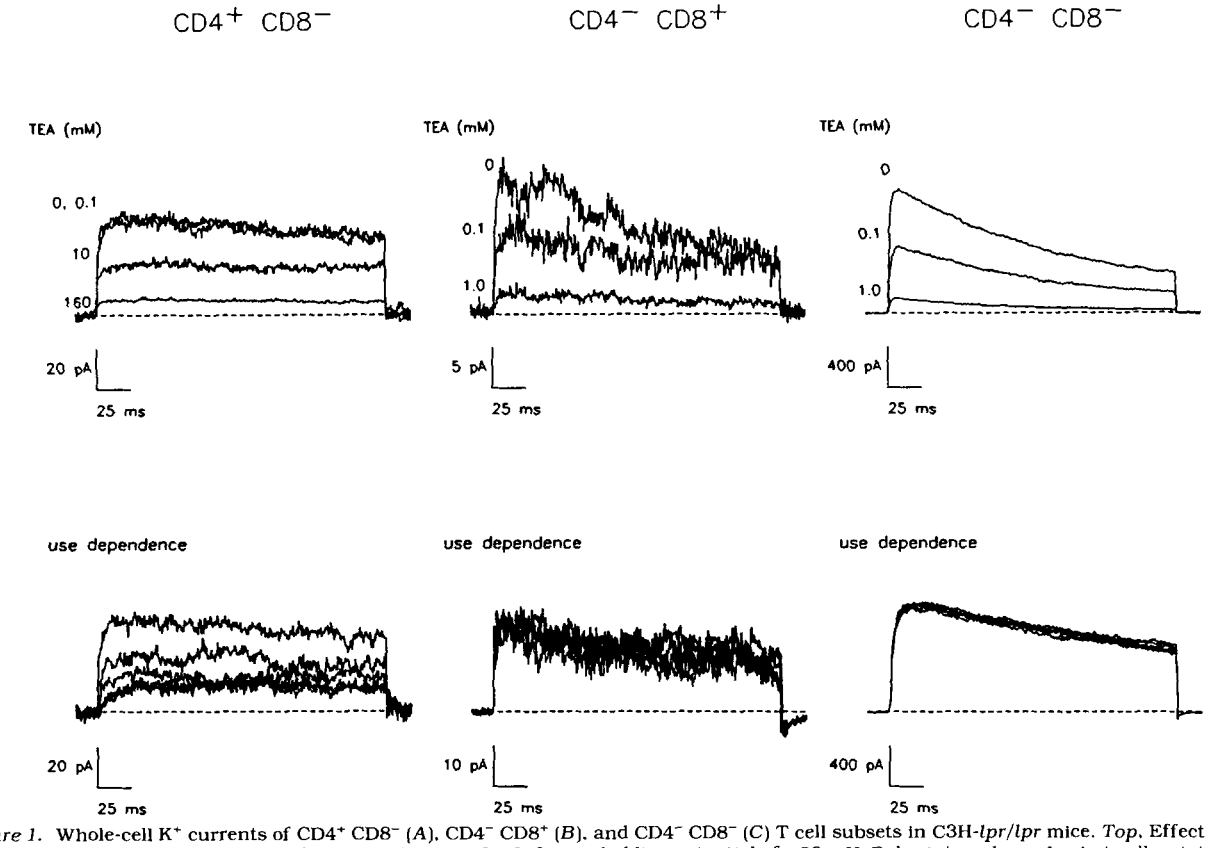

Figure 1. Whole-cell K^+ currents of $CD4^+$ $CD8^-$ (*A*), $CD4^-$ $CD8^+$ (*B*), and $CD4^-$ $CD8^-$ (*C*) T cell subsets in C3H-*lpr/lpr* mice. *Top*, Effect of TEA on K^+ currents elicited with a 200-ms depolarizing pulse to +40 mV from a holding potential of −80 mV. Pulse interval was 1 min to allow total recovery from inactivation. *Bottom*, K^+ currents were elicited as above with a pulse interval of 1 s to assay cumulative inactivation.

cell. $CD4^+$ $CD8^-$ cells (Fig. 1*A*) have small K^+ currents that are half-blocked by 10 mM TEA (*top*) and are use dependent (*bottom*), indicating that they express small numbers of type *n* K^+ channels. $CD4^-$ $CD8^+$ cells (Fig. 1*B*) display small K^+ currents that are half-blocked by 0.1 mM TEA (*top*) and are not use dependent (*bottom*), indicating that they express low levels of type *l* K^+ channels. Some $CD4^-$ $CD8^+$ cells also express small numbers of type *n'* K^+ channels (currents not shown). The abnormal $CD4^-$ $CD8^-$ T cell subset (Fig. 1*C*) has large K^+ currents that are half-blocked by 0.1 mM TEA (*top*) and are not use dependent (*bottom*), indicating that the defective cells abundantly express type *l* K^+ channels.

Figure 2*A* shows the $g_{k,max}$ in CD4- and CD8-defined T cell subsets from C3H-*lpr/lpr* mice. The abnormally proliferating $CD4^-$ $CD8^-$ T cells have a $g_{k,max}$ of 5223 ± 565 pS (mean ± SEM; n = 22). Dividing the $g_{k,max}$ by the reported single K^+ channel conductance for type *l* (3) gives an estimate of approximately 200 type *l* K^+ channels/cell, similar to the aberrant MRL-MpJ-*lpr/lpr* T cells (20). $CD4^+$ $CD8^-$ cells have a $g_{k,max}$ of 145 ± 30 pS (mean ± SEM; n = 6), representing approximately eight type *n* K^+ channels/cell. $CD4^-$ $CD8^+$ cells have a $g_{k,max}$ of 270 ± 77 pS (mean ± SEM; n = 8), representing an average of 6 to 12 type *l* or *n'* K^+ channels/cell. Thus, abundant type *l* K^+ channels are present in defective $CD4^-$ $CD8^-$ T cells from diseased C3H-*lpr/lpr* mice. In contrast, $CD4^+$ $CD8^-$ (helper/inducer) and $CD4^-$ $CD8^+$ (suppressor/cytotoxic) T cells from the lymph nodes of C3H-*lpr/lpr* mice express the same type and roughly the same numbers of K^+ channels as their phenotypically identical counterparts in the normal thymus (2, 3).

Another single-gene mutation, gld, leads to autoimmune disease and proliferation of lymph node T cells abundantly expressing type l K^+ channels. C3H-*gld/gld* develop both a lupus-like disease and the proliferation of a T cell subset phenotypically similar to that in *lpr* mice. Because the *lpr* and *gld* mutations produce the same disease, despite being non-allelic, it is conceivable that the abnormal T cells in *gld* mice have alterations of K^+ channels similar or even identical to those in C3H-*lpr/lpr* cells. Figure 2*B* demonstrates that the aberrantly proliferating $CD4^-$ $CD8^-$ T cells in C3H-*gld/gld* mice also have a large $g_{k,max}$ of 5092 ± 503 pS (mean ± SEM; n = 26), representing approximately 200 type *l* K^+ channels/cell. C3H-*gld/gld* $CD4^+$ $CD8^-$ T cells have a $g_{k,max}$ of 42 ± 3 pS (mean ± SEM; n = 5), representing approximately 2 to 3 type *n* K^+ channels/cell. $CD4^-$ $CD8^+$ T cells have a $g_{k,max}$ of 324 ± 98 pS (mean ± SEM; n = 5), indicating an average of 3 to 18 *l* or *n'* K^+ channels/cell. Thus, the abnormal $CD4^-$ $CD8^-$ T cells from sick C3H-*gld/gld* mice display a high level of type *l* K^+ channels as do the defective MRL-MpJ-*lpr/lpr* (20) and the C3H-*lpr/lpr* T cells (cf. Fig. 2*A*). On the other hand, $CD4^+$ $CD8^-$ (helper/inducer) and $CD4^-$ $CD8^+$ (suppressor/cytotoxic) T cells from the lymph nodes of these mice express a "normal" K^+ channel phenotype.

Abundant type l K^+ channels are exhibited by Thy-1.2$^+$ CD4$^-$ CD8$^-$ B220$^+$ F23.1$^+$ lymph node-derived T cells from C3H-lpr/lpr and C3H-gld/gld mice. In Figure 2, *A* and *B*, we demonstrated that the aberrant $CD4^-$ $CD8^-$ T cell subset in C3H-*lpr/lpr* and C3H-*gld/gld* mice display many type *l* K^+ channels. We examined these $CD4^-$ $CD8^-$ cells for the expression of Thy-1.2, B220, and

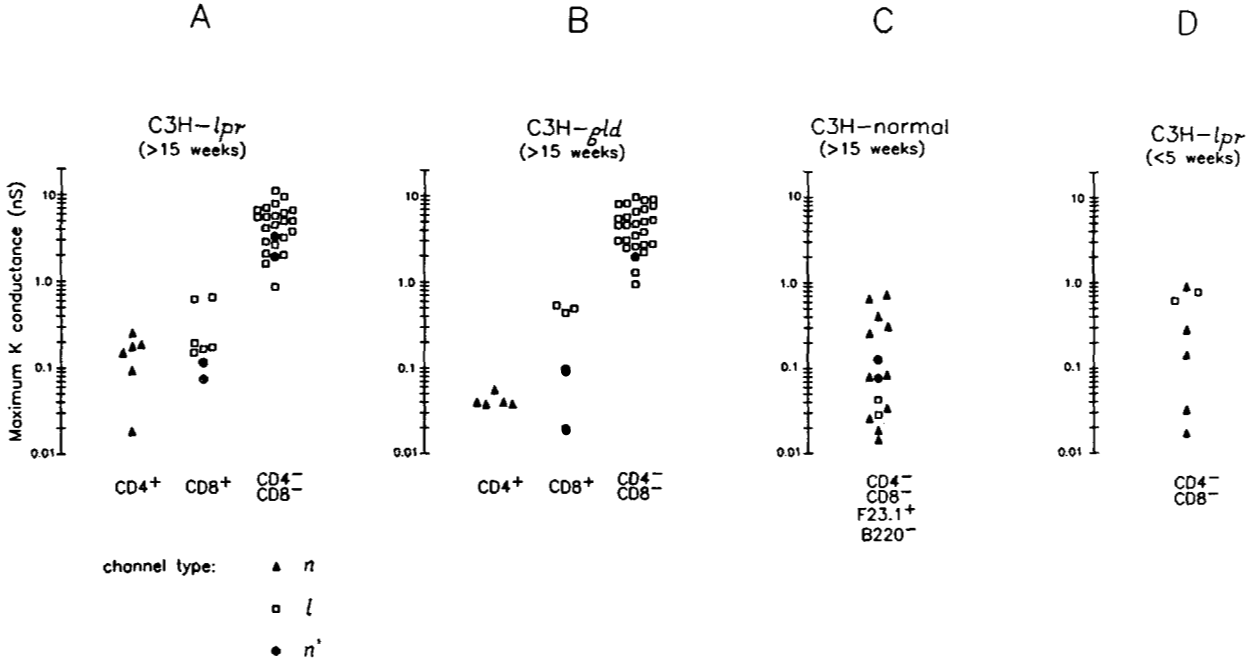

Figure 2. Maximal K^+ conductance of $CD4^+$ $CD8^-$, $CD4^-$ $CD8^+$, and $CD4^-$ $CD8^-$ T cell subsets: *A*, Diseased C3H-*lpr/lpr* mice (>15 wk old); *B*, diseased C3H-*gld/gld* mice (>15 wk old); *C*, $CD4^-$ $CD8^-$ $F23.1^+$ $B220^-$ T cells from normal C3H-HeJ mice (>15 wk old); *D*, $CD4^-$ $CD8^-$ T cells from healthy C3H-*lpr/lpr* (2 to 5 wk old). Maximal K^+ conductance reflects the number of K^+ channels per cell. The maximal K^+ conductance was measured as described in *Materials and Methods*.

F23.1 markers, which are characteristic of the diseased subset. Two experimental protocols were used.

Staining with anti-Thy-1.2-FITC and anti-CD4-PE. Figure 3 shows $g_{k,max}$ in Thy-1.2⁺ $CD4^+$ and Thy-1.2⁺ $CD4^-$ T cells from C3H-*lpr/lpr* mice. Thy-1.2⁺ $CD4^+$ cells (helper/inducer) have a $g_{k,max}$ of 144 ± 32 pS (mean ± SEM; $n = 8$), representing approximately eight type *n* K^+ channels/cell, like $CD4^+$ $CD8^-$ C3H-*lpr/lpr* T cells (cf Fig. 2*A*). Thy-1.2⁺ $CD4^-$ T cells comprise both the abnormal Thy-1.2⁺ $CD4^-$ $CD8^-$ T cells and "normal" Thy-1.2⁺ $CD4^-$ $CD8^+$ (suppressor/cytotoxic) T cells; these cells represent

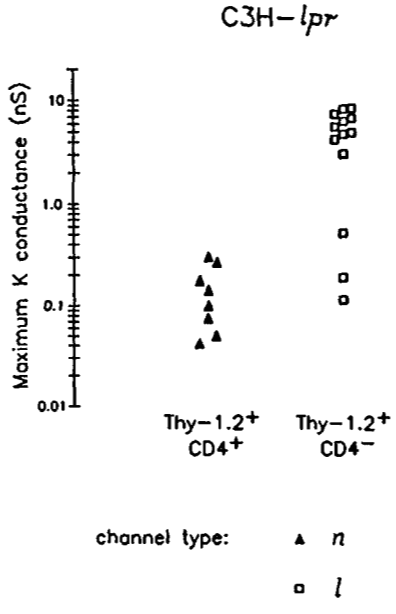

Figure 3. Maximal K^+ conductance of Thy-1.2⁺ $CD4^-$ and Thy-1.2⁺ $CD4^+$ T cells in C3H-*lpr/lpr* mice. Maximal K^+ conductance reflects the number of K^+ channels per cell. The maximal K^+ conductance was measured as described in *Materials and Methods*.

roughly 90 and 10% of the T cells of the C3H-*lpr/lpr* lymph node, respectively (8). Of 13 Thy-1.2⁺ $CD4^-$ cells examined, 10 cells (77%) had a large $g_{k,max}$ (6110 ± 545 pS, mean ± SEM; $n = 10$), indicating approximately 200 type *l* K^+ channels/cell; these cells probably represent the abnormally proliferating Thy-1.2⁺ $CD4^-$ $CD8^-$ C3H-*lpr/lpr* T cells (cf Fig. 2*A*). Of the 13 Thy-1.2⁺ $CD4^-$ cells examined, 3 (23%) had a small $g_{k,max}$ (278 ± 102 pS, mean ± SEM: $n = 3$), averaging approximately 10 type *l* K^+ channels/cell, and probably represent Thy-1.2⁺ $CD4^-$ $CD8^+$ (suppressor/cytotoxic) C3H-*lpr/lpr* T cells (cf Fig. 2*A*).

Staining voltage-clamped $CD4^-$ $CD8^-$ cells with F23.1 and B220. In the second protocol, patch-clamped $CD4^-$ $CD8^-$ cells were stained with anti-TCR antibody (F23.1) and anti-B220 antibody as described in *Materials and Methods*. All of the C3H-*lpr/lpr* ($n = 5$) and C3H-*gld/gld* ($n = 6$) $CD4^-$ $CD8^-$ cells examined were $F23.1^+$ and $B220^+$. Occasionally we found $CD4^-$ $CD8^-$ $F23.1^-$ cells in the same field as the patch-clamped cell.

We tested the specificity of this staining procedure in two ways: 1) Voltage-clamped thymocytes from normal C3H-HeJ mice did not stain with either FITC-conjugated goat anti-mouse IgG or PE-conjugated goat anti-rat IgG, the second-step reagents used in our experiments, if the cell remained viable as assessed by the stability of the K^+ currents ($n = 5$). However, the voltage-clamped cell was nonspecifically stained if the seal between the patch pipette and the clamped cell was disrupted. In all our experiments, K^+ currents remained stable after staining with anti-F23.1, anti-B220 antibodies and second-step reagents. 2) The proportion of $B220^+$ and $F23.1^+$ normal thymocytes has been reported to be approximately 5 (10) and 25% (21, 23), respectively, by flow cytometric analyses. We therefore tested our reagents on normal C3H-HeJ mouse thymocytes to determine whether the propor-

tions of B220+ and F23.1+ thymocytes detected by epifluorescence microscopy would be similar to that reported with flow cytometry. B220+ cells were evident in roughly 1% (475 cells counted) of fresh thymocytes and in 2% (492 cells counted) of F23.1+ thymocytes also stained with anti-B220 antibody. In two experiments, F23.1+ cells were found in 2% (1130 cells counted) and 9% (407 cells counted) of normal thymocytes; F23.1 staining was dim and may account for the lower percentage in our test compared with reported results obtained with flow cytometric analysis.

A phenotypically similar lymph node T cell subset from normal C3H-HeJ congenic controls does not express large numbers of type l K+ channels. A B220− thymocyte subset, otherwise phenotypically similar (Thy-1.2+ CD4− CD8− F23.1+ J11D−) to the aberrant *lpr* and *gld* cells, has recently been identified in several murine strains (23–26). Because these cells acquire B220 on activation, they have been hypothesized to be a source of the abnormal *lpr* and *gld* cells (23). A phenotypically similar lymph node T cell subset has also recently been identified (23). It is conceivable that the abundant expression of type *l* K+ channels is another cell surface feature of this novel T cell subset. We therefore examined K+ channel expression on CD4− CD8− B220− F23.1+ cells obtained from lymph nodes of normal C3H-HeJ congenic controls (see *Materials and Methods*). Figure 2*C* shows the $g_{k,max}$ of this subset. Unlike the defective *lpr* or *gld* cells (cf Fig. 2, *A* and *B*), the normal cells have a $g_{k,max}$ of 234 ± 69 pS (mean ± SEM; $n = 12$), representing approximately 12 channels/cell of either types *n*, *n'*, or *l* K+ channels or a mixture of these K+ channels. Thus, the abundant expression of type *l* K+ channels may be a feature of the diseased T cell subset in *lpr* and *gld* mice.

A phenotypically similar T cell subset from the lymph nodes and thymus of young C3H-lpr/lpr mice, obtained before the onset of disease, does not express abundant type l K+ channels. Because the number of CD4− CD8− cells increases with age in both C3H-*lpr/lpr* and C3H-*gld/gld* mice, we examined CD4− CD8− lymph node-derived T cells from 2- to 5-wk-old C3H-*lpr/lpr* mice ($n = 3$) with no overt evidence of disease. Five CD4− CD8− lymph node T cells had a $g_{k,max}$ of 275 ± 146 pS (mean ± SEM; $n = 5$) representing approximately 15 type *n* K+ channels/cell, and two cells had a $g_{k,max}$ of 704 ± 56 pS (mean ± SEM: $n = 2$), representing approximately 26 type *l* K+ channels/cell (Fig. 2*D*). In addition, eight CD4− CD8− thymocytes from these mice had a $g_{k,max}$ of 308 ± 70 pS (mean ± SEM: $n = 8$), representing approximately 17 type *n* K+ channels/cell, and two cells had a $g_{k,max}$ of 129 ± 3 pS (mean ± SEM; $n = 2$), indicating approximately 5 to 10 types *n'* or *l* channels/cell (data not shown). Thus, abnormal channel expression is a feature of the diseased CD4− CD8− T cells and is not exhibited by phenotypically similar cells before the onset of disease.

DISCUSSION

mAb-defined T cell subsets from diseased C3H-*lpr/lpr* and C3H-*gld/gld* mice and from C3H-HeJ congenic controls were investigated by using the patch clamp whole-cell recording technique. We demonstrate that the abnormally proliferating Thy-1.2+ B220+ F23.1+ CD4− CD8− T cell subset in the mutant mice displays an abundance of type *l* K+ channels, in a manner similar to that seen in MRL-MpJ-*lpr/lpr* mice (20). Phenotypically similar cells from normal congenic controls, or from young C3H-*lpr/lpr* mice examined before the onset of disease, do not express this high level of type *l* K+ channels. In contrast, CD4+ CD8− (helper/inducer) and CD4− CD8+ (suppressor/cytotoxic) T cells from both diseased strains display the same type and roughly the same number of K+ channels as their counterparts in the normal thymus.

MRL-MpJ mice develop a lupus-like syndrome late in life (6, 12). The genetic factors that contribute to the development of autoimmunity have not been identified (6, 12). However, it is clear from studies on MRL-MpJ-*lpr/lpr* mice that the *lpr* mutation accelerates the onset and severity of autoimmunity and induces severe lymphoproliferation (6). We previously reported that the abnormally proliferating T cells in MRL-MpJ-*lpr/lpr* mice exhibit numerous type *l* K+ channels (20). This altered K+ channel phenotype may be related to the expression of the *lpr* mutation alone or in combination with other genetic factors in MRL-MpJ mice. To distinguish between these possibilities, we examined ion channel expression in phenotypically similar T cells from C3H-HeJ-*lps/lps* mice that develop a disease identical to that in MRL-MpJ-*lpr/lpr* mice, although the two mice strains are genetically distinct. Furthermore, congenic control C3H-HeJ mice do not spontaneously develop this syndrome, indicating that the *lpr* mutation can induce lupus-like disease accompanied by lymphoproliferation in the absence of other genetic factors that increase susceptibility to autoimmunity. In the present study, we demonstrate that aberrant T cells from C3H-*lpr/lpr* mice exhibit large numbers of type *l* K+ channels (Figs. 2*A* and 3) as do phenotypically similar cells from diseased MRL-MpJ-*lpr/lpr* mice (20). Inasmuch as the diseased T cells from these two genetically distinct mice strains expressing the *lpr* mutation exhibit an abundance of type *l* K+ channels, the altered K+ channel phenotype is likely to be associated with the *lpr* mutation, irrespective of the genetic background of the mouse or the susceptibility of the strain to develop the lupus-like syndrome.

The *gld* mutation, although distinct from and nonallelic with the *lpr* mutation, induces hyperplasia of a phenotypically similar T cell subset (18, 19). Inasmuch as the proliferating T cells from C3H-*gld/gld* mice also display a high level of type *l* K+ channels (Fig. 2*B*) as do *lpr* T cells, it seems likely that that abundant expression of type *l* K+ channels is a marker for the aberrant T cell subset.

A novel thymocyte subset (Thy-1.2+ CD4− CD8− J11D− TCR+) has recently been identified (23–26). Unlike the abnormal *lpr* and *gld* cells, these cells do not express B220, but a variable fraction of these cells acquire B220 after activation with anti-TCR antibody plus IL-1 (23). Since these cells are phenotypically similar to the abnormally proliferating *lpr* and *gld* T cells, this subset has been hypothesized to be a source for the defective cells (23). A phenotypically identical lymph node T cell subset has also been reported (23). Recently, McKinnon and Ceredig (27) reported that this thymocyte subset, identified as CD4− CD8− J11D− thymocytes, expresses small K+ currents ($g_{k,max} = 0.5 \pm 0.3$ nS) of uncertain type. In the present study, we demonstrate that the phenotypically similar subset (CD4− CD8− B220− F23.1+) from the lymph nodes of healthy C3H-HeJ mice, displays a small number of K+ channels of types *n*, *n'*, or *l*. Furthermore, phenotypically similar cells from young

C3H-*lpr/lpr* mice tested before the onset of disease do not exhibit altered K^+ channel expression. These data imply that the abundant expression of type *l* K^+ channels by the defective $CD4^-$ $CD8^-$ *lpr* and *gld* lymph node T cells is a feature of the disease. However, it is not clear whether the abundance of type *l* K^+ channels in the *lpr* and *gld* mice reflects a causal relationship between type *l* K^+ channels and abnormal proliferation or whether it is a manifestation of the disease.

The defective *lpr* and *gld* T cells do not express the IL-2R nor do they produce IL-2, molecules normally expressed by lectin- and Ag-activated T cells (13, 19). Furthermore, lectin- and Ag-activated T cells display a large number of type *n* K^+ channels (5, 20), in contrast to the abundance of type *l* K^+ channels expressed by the diseased *lpr* and *gld* cells. Taken together, these data suggest that a proliferative signal, distinct from the normal lectin- and Ag-activated pathway, causes the hyperplasia of those defective T cells that abundantly express type *l* K^+ channels.

Palacios (28) reported that spleen cells from MRL-MpJ-*lpr/lpr* mice constitutively produce an IL-3-like activity when tested on an IL-3-dependent pre-B cell line and suggested that this lymphokine may be responsible for the lymphoid hyperplasia in these mice. In contrast, Kelley and colleagues (29) did not confirm this result with spleen cells from MRL-MpJ-*lpr/lpr* mice or three other mouse strains bearing the mutant *lpr* gene either by the bioassay or by measuring IL-3 mRNA. However, two recent reports by Ohta et al. (30, 31) indicate that, although lymphoid cells from MRL-MpJ-*lpr/lpr* mice do not constitutively secrete an IL-3-like substance, sera from these diseased mice contain IgG with IL-3-like activity. B cell hybridomas that secrete mAb with IL-3-like activity have been established from sick MRL-MpJ-*lpr/lpr* mice (31). Based on these data, the authors conclude that lymphoid hyperplasia in mice bearing the *lpr* mutation may result from stimulation by autoantibodies directed against the IL-3-R. It is therefore conceivable that IL-3 or one of the newly identified lymphokines induces hyperplasia of $CD4^-$ $CD8^-$ T cells from *lpr* and *gld* mice, the abundant expression of type *l* K^+ channels reflecting excessive stimulation via lymphokine-specific receptors.

Acknowledgments. The authors are indebted to Dr. Sudhir Gupta, Chief, Division of Basic and Clinical Immunology, for his continued support, Mr. Robert Spencer for excellent technical assistance, and Ms. Ruth Davis for proofreading this manuscript. We thank Mr. John Roths for making these mice strains available to us. We are especially grateful to Dr. Charles Sidman for his excellent comments about our manuscript.

REFERENCES

1. **DeCoursey, T. E., K. G. Chandy, S. Gupta, and M. D. Cahalan.** 1987. Two types of potassium channels in murine T lymphocytes. *J. Gen. Physiol 89:379.*
2. **Lewis, R. S., and M. D. Cahalan.** 1987. Diversity of K^+ channel expression in developing T lymphocytes. *J. Gen. Physiol 90:27a.*
3. **Lewis, R. S., and M. D. Cahalan.** 1988. Subset-specific expression of potassium channels in developing murine T lymphocytes. *Science 239:771.*
4. **DeCoursey, T. E., K. G. Chandy, S. Gupta, and M. D. Cahalan.** 1985. Voltage-dependent ion channels in T lymphocytes. *J. Neuroimmunol. 10:71.*
5. **DeCoursey, T. E., K. G. Chandy, S. Gupta, and M. D. Cahalan.** 1987. Mitogen induction of K^+ channels in murine T lymphocytes. *J. Gen. Physiol 89:405.*
6. **Murphy, E. D.** 1981. Lymphoproliferation (*lpr*) and other single locus models of murine lupus. In *Immunologic Defects in Laboratory Animals*, Vol. 2. M. E. Gershwin and B. Merchant, eds. Plenum Press, New York, pp. 143–173.
7. **Nemazee, D. A., S. Studer, M. Steinmetz, Z. Dembic, and M. Kiefer.** 1985. The lymphoproliferating cells of the MRL-*lpr/lpr* mice are a polyclonal population that bear the lymphocyte receptor for antigen. *Eur. J. Immunol. 15:760.*
8. **Davidson, W. F., F. J. Dumont, H. G. Bedigian, B. J. Fowlkes, and H. C. Morse III.** 1986. Phenotypic functional, and molecular genetic comparisons of the abnormal lymphoid cells of C3H-*lpr/lpr* and C3H-*gld/gld* mice. *J. Immunol. 136:4075.*
9. **Hashimoto, Y., Y. Katsuyuki, D. Littman, and M. I. Greene.** 1987. T-cell receptor genes in autoimmune mice: T-cell subsets have unexpected T-cell receptor gene programs. *Proc. Natl. Acad. Sci. USA 84:5883.*
10. **Budd, R. C., M. Schreyer, G. S. Miescher, and H. R. MacDonald.** 1987. T cell lineages in the thymus of *lpr/lpr* mice: evidence for parallel pathways of normal and abnormal T cell development. *J. Immunol. 139:2200.*
11. **Theofilopoulos A. N., R. A. Eisenberg, M. Bourdon, J. S. Crowell, and F. J. Dixon.** 1979. Distribution of lymphocytes identified by surface markers in murine strains with systemic lupus erythematosus-like syndromes. *J. Exp. Med. 149:516.*
12. **Lewis D. E., J. V. Giorgi, and N. L. Warner.** 1981. Flow cytometry analysis of T cells and continuous T-cell lines from autoimmune MRL/l mice. *Nature 289:298–300.*
13. **Morse, H. C. III., W. F. Davidson, R. A. Yetter, E. D. Murphy, J. B. Roths, and R. L. Coffman.** 1982. Abnormalities induced by the mutant gene *lpr*: expansion of a unique lymphocyte subset. *J. Immunol. 129:2612.*
14. **Wofsy, D., R. R. Hardy, and W. E. Seaman.** 1984. The proliferating cells in autoimmune MRL/*lpr* mice lack L3T4, an antigen on "helper" T cells that is involved in the response of class II major histocompatibility antigens. *J. Immunol. 132:2686.*
15. **Steinberg, A. S., D. P. Huston, J. D. Taurog, J. S. Cowdery, and E. S. Raveche.** 1981. The cellular and genetic basis of murine lupus. *Immunol. Rev. 55:121.*
16. **Izui, S., V. E. Kelley, K. Masuda, Y. Yoshida, J. B. Roths, and E. D. Murphy.** 1984. Induction of various auto-antibodies by mutant gene *lpr* in several strains of mice. *J. Immunol. 133:227.*
17. **Roths, J. B.** 1987. Differential expression of murine autoimmunity and lymphoid hyperplasia determined by single genes. In *New Horizons in Animal Models for Autoimmune Disease.* H. Wigzell and M. Kyogoku, eds. Academic Press, Tokyo.
18. **Roths, J. B., E. D. Murphy, and E. M. Eicher.** 1984. A new mutation, *gld*, that produces lymphoproliferation and autoimmunity in C3H-HeJ mice. *J. Exp. Med 159:1.*
19. **Davidson, W. F., K. L. Holmes, J. B. Roths, and H. C. Morse III.** 1985. Immunologic abnormalities of mice bearing the *gld* mutation suggest a common pathway for murine non-malignant lymphoproliferative disorders with autoimmunity. *Proc. Natl. Acad. Sci. USA 82:1219.*
20. **Chandy, K. G., T. E. DeCoursey, M. Fischbach, N. Talal, M. D. Cahalan, and S. Gupta.** 1986. Altered K^+ channel expression in abnormal T lymphocytes from mice with the *lpr* gene mutation. *Science 233:1197.*
21. **Staerz, U. D., H. G. Rammensee, J. D. Benedetto, and M. J. Bevan.** 1985. Characterization of a murine monoclonal antibody specific for an allotypic determinant on T cell antigen receptor. *J. Immunol. 134:3994.*
22. **Cahalan, M. D., K. G. Chandy, T. E. DeCoursey, and S. Gupta.** 1985. A voltage-gated K^+ channel in human T lymphocytes. *J. Physiol. 358:197.*
23. **Fowlkes, B. J., A. M. Kruisbeek, H. Ton-That, M. A. Weston, J. E. Coligan, R. H. Schwartz, and D. M. Pardoll.** 1987. A novel population of T-cell receptor $\alpha\beta$-bearing thymocytes which predominantly expresses a V_β gene family. *Nature* 329:251.
24. **Budd, R. C., G. Miescher, R. C. Howe, R. K. Lees, C. Bron, and H. R. MacDonald.** 1987. Developmentally regulated expression of T-cell receptor β chain variable domains in immature thymocytes. *J. Exp. Med. 166:577.*
25. **Ceredig, R., F. Lynch, and P. Newman.** 1987. Phenotypic properties, interleukin 2 production, and developmental origin of a "mature" subpopulation of $Lyt\text{-}2^-$ $L3T4^-$ mouse thymocytes. *Proc. Natl. Acad. Sci. USA 84:8578.*
26. **Crispe, I. N., M. W. Moore, L. A. Husmann, L. Smith, M. J. Bevan, and R. P. Shimonkevitz.** 1987. Differentiation potential of subsets of $CD4^-$ $CD8^-$ thymocytes. *Nature 329:336.*
27. **McKinnon, D., and R. Ceredig.** 1986. Changes in the expression of potassium channels during mouse T-cell development. *J. Exp. Med. 164:1846.*
28. **Palacios, R.** 1984. Spontaneous production of interleukin-3 by T lymphocytes from autoimmune MRL/MpJ-*lpr/lpr* mice. *Eur. J. Immunol. 14:599.*
29. **Kelley, V. E., N. M. Farber, J. M. Williams, and T. B. Strom.** 1986. Inability of autoimmune mice with the *lpr* gene to spontaneously produce interleukin-3. *Eur. J. Immunol. 16:464.*
30. **Ohta, Y., S. Tamura, E. Tezuka, M. Sugawara, S. Imai, and H. Tanaka.** 1988. Autoimmune MRL/*lpr* mice sera contain IgG with interleukin 3-like activity. *J. Immunol. 140:520.*
31. **Sugawara, M., C. Hattori, E. Tezuka, S. Tamura, and Y. Ohta.** 1988. Monoclonal autoantibodies with interleukin 3-like activity derived from a MRL/*lpr* mouse. *J. Immunol. 140:526.*